

Article

The Response of Regeneration Ability of *Myriophyllum spicatum* Apical Fragments to Decaying *Cladophora oligoclona*

Lu Zhang ^{1,2}, Suzhen Huang ², Xue Peng ², Biyun Liu ^{2,*} , Yi Zhang ², Qiaohong Zhou ² and Zhenbin Wu ^{1,2}

¹ School of Resource and Environmental Engineering, Wuhan University of Technology, Wuhan 430070, China; s050zhanglu@163.com (L.Z.); wuzb@ihb.ac.cn (Z.W.)

² State Key Laboratory of Freshwater Ecology and Biotechnology, Institute of Hydrobiology, Chinese Academy of Sciences, Wuhan 430072, China; huangsuzhenlmy@163.com (S.H.); 18702742827@163.com (X.P.); zhangyi@ihb.ac.cn (Y.Z.); qhzhou@ihb.ac.cn (Q.Z.)

* Correspondence: liuby@ihb.ac.cn; Tel.: +86-027-687-800-38

Received: 15 March 2019; Accepted: 10 May 2019; Published: 15 May 2019



Abstract: During the restoration of eutrophic shallow lakes, submerged macrophyte recovery is often accompanied by an excessive proliferation of filamentous green algae (FGA). This can lead to the recession or even disappearance of the submerged macrophytes in these lakes. However, the use of plant fragments in reproduction and dispersion is an important life history strategy for submerged macrophytes. In this work, it studied apical fragment propagation in *Myriophyllum spicatum* and its physiological and biochemical responses to the decomposing liquid of *Cladophora oligoclona*. *Myriophyllum spicatum* apical fragments showed no new roots or buds when treated with 0.4 times the original decomposing liquid, and their PSII functional parameters were lower than those of the control. In contrast, the relevant sugar content accumulated to 115.26%, and the activities of an energy enzyme ($\text{Ca}^{2+}/\text{Mg}^{2+}$ -ATPase) and a secondary metabolic-related enzyme (PAL) increased by 490.63% and 28.13%, showing an elevated defense response. These results indicated that the early regeneration of *M. spicatum* could be hindered by environmental stress, and that this may further affect the reproduction and colonization of these submerged macrophytes.

Keywords: apical fragment; *Cladophora oligoclona*; decomposing liquid; *Myriophyllum spicatum*; regeneration

1. Introduction

Lake eutrophication is a serious and pervasive environmental problem that threatens the health and stability of aquatic ecosystems [1,2]. Lake eutrophication leads to the decline of submerged macrophytes, and succession from a macrophyte-dominated to an algae-dominated ecosystem [3]. The restoration of submerged macrophytes is an important method of artificially regulating the transformation of algae-dominated lakes into macrophyte-dominated lakes through external controls [4,5]. The growth and reproductive abilities of submerged macrophytes are highly significant in the reconstruction and restoration of these species. Submerged macrophytes prioritize asexual reproduction using fragments, stolons, and rhizomes. Moreover, the use of fragments for reproduction and dispersion is an important life history strategy for submerged macrophytes when responding to environmental disturbances [6,7]. The fragments can produce new plants for colonization and regeneration which affect population establishment and renewal [8]. Therefore, it is important to study the growth and regeneration strategies of these fragments under different conditions.

During the early stages of submerged macrophyte recovery in eutrophic lake restoration, when the lake system has not yet reached a stable state, a phenomenon often occurs in which a large amount of

filamentous green algae (FGA) grows [9]. These FGA tend towards excessive growth and the formation of thick floating algae mats under suitable environmental conditions, and can lead to the decline or even disappearance of submerged macrophytes [10]. As well as mechanically damaging their stems and leaves by twining around them, FGA competes with submerged macrophytes for space, light, nutrients, and other resources [11], negatively influencing their normal growth. Once the large biomass of FGA reaches senescence, it begins to decompose over a large area and leads to deterioration of the water quality in a short period of time [12]. To make matters worse, it continuously releases phenolic acids and aromatic organic pollutants during decomposition [13–15]. Meanwhile, a large amount of nutrients infiltrate the water body, increasing the degree of eutrophication and potentially leading to the growth of harmful microalgae or algal blooms [16,17]. The previous research found that decaying *Cladophora oligoclona* had a great impact on *Hydrilla verticillata* seed germination and seedling growth, and is not conducive to the expansion and reproduction of submerged macrophytes [18]. However, it is not yet clear whether the decomposition of FGA will affect the growth of different propagules of submerged macrophytes, and there is still little information about the physiological and biochemical responses to the decomposing liquid of FGA in the asexual reproduction of submerged macrophytes. Moreover, there is even less comprehensive research on the relationships between the responses of submerged macrophytes and environmental stress factors.

Myriophyllum spicatum is a perennial submerged macrophyte of the *Haloragidaceae* family. Due to its strong resistance to pollution, *M. spicatum* is one of the pioneer species used in the aquatic vegetation restoration projects [19]. Because of environmental disturbances such as wave action, herbivory, boating, and so forth, *M. spicatum* is easily broken to form apical fragments [20,21]. As the fragments float in the upper level of the water column, the impacts of limited dissolved oxygen and light intensity are reduced. It is thus possible for the fragments to develop into robust new plants and gradually settle to form colonies. Fragments from parent plants are therefore one of the most important methods of reproduction for *M. spicatum* under natural conditions. Previous research reported that the apical fragments had better adventitious root and bud formation abilities [8,22]. Hence, during eutrophic lake recovery, *M. spicatum* fragmentations are considered an effective method of asexual reproduction and are helpful for the spread of *M. spicatum* from single individuals into communities [23,24].

The rooting and sprouting of plant fragments during regeneration could be affected by environmental stresses such as pH, light, turbidity, and nutrients [25–28]. During plant growth and regeneration, photosynthesis is an extremely important metabolic process, and its intensity also has a very important influence on growth and stress resistance [29,30]. In order to present the actual physiological state of the PSII photosynthetic system, based on chloroplast biofilm flow, the JIP test, which has proved to be a useful tool for the *in vivo* investigation of PSII function under various environmental stresses, was used to analyze the rapid chlorophyll *a* fluorescence induction curve (OJIP) and its parameters [31,32]. When plants are exposed to environmental stress, not only the photosynthetic system of the plant is damaged, but the physiological and biochemical state of the plant also responds and changes. For example, stressed plants often accumulate sugar and other carbohydrates to provide energy, and the related membrane energy enzymes such as $\text{Ca}^{2+}/\text{Mg}^{2+}$ -ATPase are also activated. $\text{Ca}^{2+}/\text{Mg}^{2+}$ -ATPase regulates Ca^{2+} levels in the cytosol pool to maintain the cytoplasmic Ca^{2+} homeostasis required for normal protein synthesis and cell growth [33,34]. Meanwhile, the secondary metabolites in facilitating secondary metabolic activities will be increased to enhance resistance [35,36]. Phenylalanin ammo-nialyase (PAL) is an important secondary metabolic defense enzyme in plant stress resistance and could form various antibacterial products such as phenols, flavonoids, and salicylic acid in the phenylpropanoid metabolic pathway [37].

In order to avoid interference from the physical winding and shading of decaying FGA, decomposing liquid was adopted in this experiment. The apical fragments of *M. spicatum* were treated in different concentrations of *C. oligoclona* decomposing liquid, and the JIP test parameters, chlorophyll *a* content, soluble sugar content, and $\text{Ca}^{2+}/\text{Mg}^{2+}$ -ATPase and PAL activities were determined. It hypothesized that the regeneration abilities of apical fragments of *M. spicatum* would change significantly according to

the concentration of the decomposing liquid because higher concentrations of the decomposing liquid would lead to changes in water quality, and induce various physiological and biochemical responses in the apical fragments, inhibiting their regeneration abilities. The aims of this research are to assess: (1) the effects of decomposing liquid on the roots and buds of *M. spicatum* apical fragments; (2) the responses of the apical fragment's photosynthetic systems to decomposing liquid; (3) the responses of the energy content and secondary metabolism of the apical fragments to decomposing liquid; (4) the impacts of decomposing liquid on the living environment of the apical fragments, including changes of pH, dissolved oxygen (DO), and conductivity (Cond), and their relationship to the physiological and biochemical characteristics of the apical fragments.

2. Materials and Methods

2.1. Material Collection and Experimental Design

For the purpose of clarifying the response of different propagules to the decaying FGA, *C. oligoclona* and *M. spicatum* were collected from East Lake, Wuhan, China (30°55' N, 114°36' E) (mesotrophic lake, pH: 6~9, COD $\leq 20 \text{ mg}\cdot\text{L}^{-1}$, DO $\geq 5 \text{ mg}\cdot\text{L}^{-1}$) in February and April 2017, respectively. The collected *C. oligoclona* was used for the production of decomposing liquid. The preparation method of the decomposing liquid of *C. oligoclona*, and the treatments concentrations used in this study were based on a previous study [18]. All *C. oligoclona* was decomposed in a constant 25 °C environment and protected from light. Healthy *M. spicatum* plants with intact leaves were selected and any impurities were washed off with pure water. Next, 10 cm length apical fragments were cut for use.

The four treatment concentrations were: control group (CG, without decomposing liquid), Treatment No. 1 (T1, 0.1 times the concentration of the original decomposing liquid), Treatment No. 2 (T2, 0.2 times the concentration of the original decomposing liquid), and Treatment No. 3 (T3, 0.4 times the concentration of the original decomposing liquid). These concentrations reflect the average biomass of *Cladophora* in a eutrophic lake in spring [38]. Considering the better implementation of laboratory experiments, it took 0.1 of the average biomass as the material for the original decomposing liquid ($50 \text{ g}\cdot\text{L}^{-1}$), and then selected a few concentrations within the range of the original decomposing liquid which represent different degrees of decomposition by *C. oligoclona* at this density, allowing us to analyze the effects of decomposing liquid on submerged macrophytes more comprehensively. Six apical fragments without adventitious roots or buds were cultivated in each flask. All treatments were performed in triplicate. The experiment was carried out at an ambient temperature of $25 \pm 1 \text{ }^\circ\text{C}$ and an irradiance of 2000 lx under a 12:12 h light–dark cycle.

2.2. Physiological and Biochemical Analyses of Apical Fragment

The morphological traits of the adventitious roots and buds were measured on day 5, and buds longer than 3 mm were recorded as occurrences. On days 1, 3, and 5, various indicators were measured including the chlorophyll *a* content, soluble sugar, $\text{Ca}^{2+}/\text{Mg}^{2+}$ -ATPase, and PAL activity of the apical fragments and the water quality. The water quality parameters—including pH, Cond, and DO—were measured with an online analyzer (Thermo Orion star A329, USA).

Under conditions of $25 \pm 1 \text{ }^\circ\text{C}$ and 10 min dark adaptation, a Handy PEA (Hansatech, England) was used to measure chlorophyll *a* fluorescence in the top 2–3 cm of the apical fragments. For each treatment, three apical fragments were selected randomly for the parallel measurement of chlorophyll *a* fluorescence and the readings were taken three times. The Handy PEA instrument automatically recorded high-resolution interstitial fluorescence signals from 10 μs to 2 s and automatically derived the relevant fluorescence parameters. In order to better observe the J-step and the I-step in the plot of the OJIP fluorescence induction curve, the abscissa representing the time is generally changed to a logarithmic coordinate before the OJIP induced curve is obtained. Based on the method proposed by Schansker et al. [39], the OJIP fluorescence induction curve was analyzed using a JIP test. The JIP test parameters quantifying PSII behavior were obtained and calculated as shown in Table 1 [40].

Table 1. Formulas and terms used in the JIP-test.

Parameter	Implication
$F_M = F_P$	The maximal fluorescence intensity at P step.
F_I	The fluorescence intensity at 30 ms (I-step).
F_J	The fluorescence intensity at 2 ms (J-step).
F_0	The fluorescence intensity at 50 μ s (O-step).
V_J	Relative variable fluorescence intensity at the J-step.
M_0	Approximated initial slope of the fluorescence transient.
$ABS/RC = (M_0/V_J) (1/\varphi_{P_0})$	Absorption flux per RC.
$TR_0/RC = M_0/V_J$	Trapped energy flux per RC.
$ET_0/RC = (M_0/V_J) \psi_0$	Electron transport flux per RC.
$DI_0/RC = ABS/RC - TR_0/RC$	Dissipated energy flux per RC.
$\varphi_{P_0} = [1 - (F_0/F_M)] = F_V/F_M$	Maximum quantum yield for primary photochemistry.
$\varphi_{E_0} = [1 - (F_0/F_M)] \psi_0$	Quantum yield for electron transport.
$\psi_0 = 1 - V_J$	Probability that a trapped exciton moves an electron into the electron transport chain beyond Q_A^- .
$RC/CS = F_0 \cdot \varphi_{P_0} \cdot V_J / M_0$	Density of RCs.
$PI_{ABS} = (RC/ABS) [\varphi_{P_0}(1 - \varphi_{P_0})] [\psi_0(1 - \psi_0)]$	Performance index on absorption basis.
F_V/F_M	Maximum photochemical efficiency.
$V_J = (F_{2ms} - F_0)/(F_M - F_0); M_0 = 4(F_{300\mu s} - F_0)/(F_M - F_0)$	

The ethanol extraction method was adopted to determine the content of chlorophyll *a* in the fresh leaves of the apical fragments [41]. Anthrone reagent was used to determine the soluble sugar content, according to Yemm and Willis [42]. A kit (Suzhou Keming Bioengineer Company, China) was used to determine the activity of Ca^{2+}/Mg^{2+} -ATPase, and the activity of PAL was measured according to Sykłowska-Baranek et al. [43] and Zhang et al. [18]. The activities of the two enzymes were determined according to the content of the proteins [44].

2.3. Data Analysis

Statistical analyses were performed in SPSS 23.0 using one-way analysis of variance (ANOVA). All data are presented as the mean value and standard deviation (mean \pm SD), and the sample number (n) was three. The Bonferroni post hoc test was applied for pairwise comparisons, and the Tukey's honest significant difference test was used to test for differences between means. Differences were considered statistically significant at $P < 0.05$.

The correlations between the physiological and biochemical characteristics of *M. spicatum* apical fragments and water quality parameters were analyzed using CANOCO 4.5. First, detrended correspondence analysis was performed. The obtained sorting axis gradient length (LGA) was used to reflect the degree of change in the physiological and biochemical characteristics of the apical fragments. In theory, an LGA < 3 is suitable for linear models, an LGA > 4 is suitable for nonlinear models, and an LGA between 3 and 4 indicates that both models are suitable [45]. The analysis in this study showed that the maximum LGA of the four sorting axes was 0.600 (less than 3), indicating that the physiological and biochemical characteristics of the apical fragments have a good linear response to the water quality parameters. Therefore, it is appropriate to use a linear model for redundancy analysis (RDA). RDA is an extension of multiple linear regression, a type of multivariate direct gradient analysis [46]. It can be used to analyze the linear relationship between two sets of variables and reflect, on the same axis, the relationship between the physiological and biochemical characteristics of *M. spicatum* and the water quality parameters. Meanwhile, the Monte Carlo permutation test was used to quantitatively and independently evaluate the influence of the water quality parameters on the changes of physiological and biochemical characteristics of the apical fragment.

3. Results

3.1. Effects of the Decomposing Liquid on Apical Fragments Adventitious Roots and Buds

The mean adventitious root length and number, and bud number, of *M. spicatum* apical fragments under the different treatments all showed significant differences ($P < 0.001$, $P < 0.001$, $P < 0.001$, ANOVA, Figure 1). The average adventitious root length in CG was the longest. The trend in the adventitious root length among the treatments was the same as that of the root number, and no adventitious roots were generated in the T3 treatment group during the experimental period. Compared to CG, bud production was significantly inhibited in the two higher concentration groups (T2, T3) ($P < 0.05$, $P < 0.05$, Bonferroni), and the bud number in T1 was also lower than that in CG. At the late stage of the experiment, no roots appeared in T3, the leaves of the apical fragments were black, some lower leaves fell off, black attachments on the apical fragments indicated that rooting and bud germination was affected, and some tissues began to decompose.

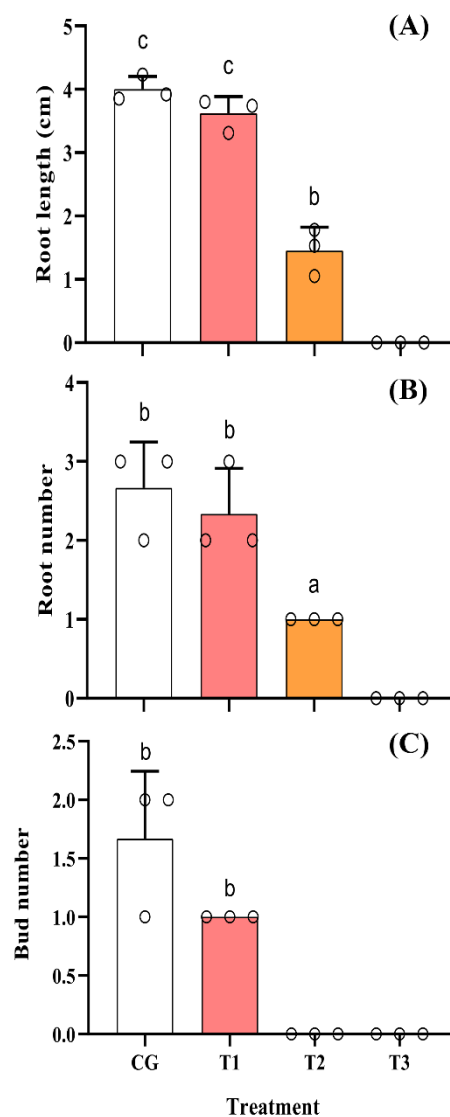


Figure 1. The mean adventitious root length (A) and number (B), and bud number (C) of *M. spicatum* in each treatment on day 5 (data points). CG: control group; T1: 0.1 times of original decomposing liquid; T2: 0.2 times of original decomposing liquid; T3: 0.4 times of original decomposing liquid. Error bars represent standard deviation (n = 3). The different letters on top of the columns indicate significant differences among treatments at the 0.05 significance level (Tukey HSD). Each dot represents a replicate.

3.2. Changes of Chlorophyll a Content and Chlorophyll Fluorescence Characteristics

The OJIP fluorescence induction curve in Figure 2 displayed an obvious trend of different treatment groups from day 1 to day 5. Especially from the J phase, the OJIP curve of *M. spicatum* apical fragment leaves in T1, T2, and T3 showed a descending trend compared to CG in the whole experimental phase, and the difference between T3 and CG was significant on day 5 ($P < 0.05$, Bonferroni) (Figure 2A). As the concentration of the decomposing liquid increased, the fluorescence values of I and P phases (maximal recorded fluorescence intensity) decreased, by 22.91 and 36.31%, 45.81 and 26.25%, and 40.42 and 50.00% by the end of experiment in T1, T2, and T3, respectively. The decreases in the I-P phases indicate that the presence of the decomposing liquid affects the photosynthetic mechanism.

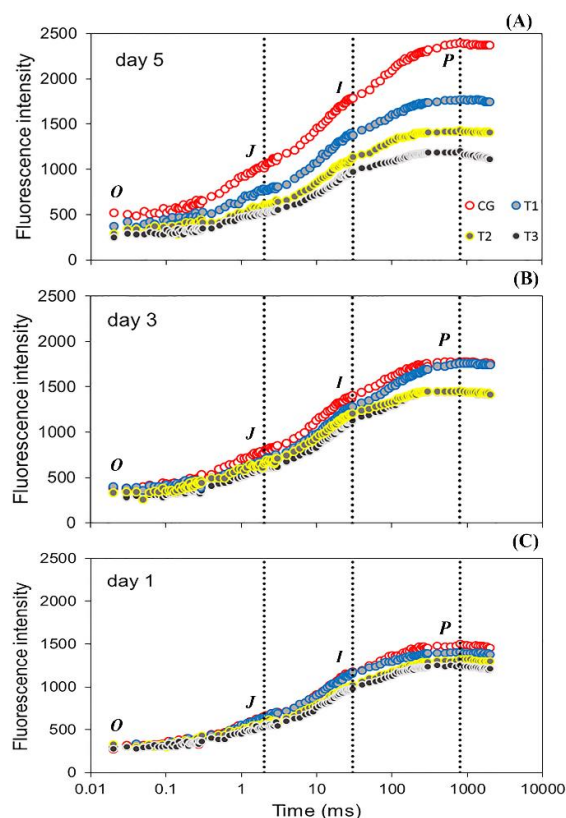


Figure 2. Representative OJIP curves for *M. spicatum* in each treatment on day 1 (C), 3 (B), and 5 (A). CG: control group; T1: 0.1 times of original decomposing liquid; T2: 0.2 times of original decomposing liquid; T3: 0.4 times of original decomposing liquid.

F_V/F_M and PI_{ABS} in CG both increased as the experiment went on. However, F_V/F_M showed a decreasing trend in T2 and T3, and their F_V/F_M ratios were 4.94% and 7.41% lower than that in CG on day 5. The differences between T1 (T2, T3) and CG were significant ($P < 0.01$, $P < 0.001$, $P < 0.001$, Bonferroni). The PI_{ABS} of CG and T1 showed a continuous increasing trend, while that of T2 and T3 showed a more varied trend, first increasing on day 3 and then decreasing on day 5. The decrease was associated with the concentration of the decomposing liquid; the higher the concentration, the lower the value. Compared with CG, the decreases in T2 and T3 were significant and had decreased by 43.76% and 47.45% after 5 days ($P < 0.01$, $P < 0.001$, Bonferroni) (Table 2). As can be seen from Table 2, the ABS/RC and TR_o/RC in CG and T1 rose initially before falling, while in T2 and T3 they rose continuously over time. Similar changes were also reflected in ϕ_{Eo} and ψ_o . However, these continued to descend until the end of the experiment in T2 and T3. After 5 days, ET_o/RC (which related to the reoxidation of reduced Q_A via electron transport in an active RC) and DI_o/RC in T1, T2 and T3 increased 4.67, 4.00 and 13.56, 1.67, 2.33, and 27.67 times than that in CG, respectively. In contrast, RC/CS (The density of RC_S) decreased by 28.94%, 90.48%, and 94.89%, respectively.

Table 2. JIP-test parameters for *M. spicatum* fragments leaf under different concentration decomposing liquid of *C. oligoclona* for different time periods.

Parameter	CG			T1			T2			T3		
	1d	3d	5d	1d	3d	5d	1d	3d	5d	1d	3d	5d
PI _{ABS}	3.93 ± 0.99a	4.84 ± 0.56a	5.69 ± 0.44b	2.84 ± 0.35a	5.00 ± 0.57a	5.46 ± 0.07b	2.35 ± 0.09a	4.61 ± 0.41a	3.20 ± 1.01a	2.28 ± 0.20a	4.10 ± 0.09a	2.99 ± 0.59a
φ _{E0}	0.64 ± 0.01b	0.66 ± 0.03b	0.63 ± 0.02b	0.58 ± 0.03a	0.65 ± 0.03b	0.62 ± 0.00b	0.63 ± 0.02ab	0.61 ± 0.01ab	0.61 ± 0.01b	0.59 ± 0.03ab	0.58 ± 0.02a	0.53 ± 0.04a
ψ ₀	0.77 ± 0.02a	0.80 ± 0.01a	0.82 ± 0.03b	0.75 ± 0.03a	0.82 ± 0.04a	0.79 ± 0.00ab	0.81 ± 0.02a	0.80 ± 0.03a	0.78 ± 0.02ab	0.78 ± 0.03a	0.75 ± 0.02a	0.74 ± 0.05b
V _J	0.24 ± 0.02b	0.18 ± 0.03a	0.20 ± 0.01a	0.25 ± 0.03b	0.19 ± 0.04a	0.21 ± 0.00a	0.19 ± 0.02b	0.20 ± 0.03a	0.22 ± 0.02ab	0.10 ± 0.01a	0.22 ± 0.03a	0.25 ± 0.02b
M ₀	0.04 ± 0.00a	0.13 ± 0.05ab	0.03 ± 0.01a	0.08 ± 0.01ab	0.05 ± 0.00a	0.03 ± 0.00a	0.17 ± 0.06c	0.15 ± 0.04b	0.27 ± 0.00b	0.12 ± 0.03bc	0.13 ± 0.02b	0.26 ± 0.04b
F _V /F _M	0.79 ± 0.01b	0.79 ± 0.00b	0.81 ± 0.01d	0.77 ± 0.01ab	0.79 ± 0.00b	0.79 ± 0.00c	0.77 ± 0.01ab	0.78 ± 0.02ab	0.77 ± 0.00b	0.76 ± 0.00a	0.76 ± 0.00a	0.75 ± 0.00a
ABS/RC	0.25 ± 0.02a	0.65 ± 0.10ab	0.17 ± 0.08a	0.29 ± 0.09b	0.35 ± 0.07b	0.20 ± 0.01a	0.86 ± 0.20c	0.88 ± 0.11b	1.25 ± 0.04b	1.12 ± 0.17c	1.58 ± 0.04c	2.12 ± 0.23c
TR ₀ /RC	0.18 ± 0.02a	0.52 ± 0.05b	0.14 ± 0.06a	0.23 ± 0.07a	0.28 ± 0.08a	0.16 ± 0.01a	0.74 ± 0.06b	0.82 ± 0.02c	0.92 ± 0.06b	0.92 ± 0.05d	1.10 ± 0.10ab	1.27 ± 0.60b
ET ₀ /RC	0.15 ± 0.01a	0.39 ± 0.04bc	0.09 ± 0.02a	0.19 ± 0.04a	0.22 ± 0.04a	0.42 ± 0.05b	0.62 ± 0.08b	0.54 ± 0.16c	0.36 ± 0.03b	0.71 ± 0.00b	0.33 ± 0.01ab	1.22 ± 0.08c
DI ₀ /RC	0.04 ± 0.00a	0.14 ± 0.03b	0.03 ± 0.00a	0.07 ± 0.02a	0.06 ± 0.01a	0.05 ± 0.00a	0.22 ± 0.04b	0.19 ± 0.02c	0.21 ± 0.01b	0.29 ± 0.01b	0.14 ± 0.02b	0.83 ± 0.04c
RC/CS	1870.65 ± 59.61c	727.26 ± 19.50b	3607.86 ± 634.96	1148.41 ± 65.16b	1236.07 ± 117.85c	2563.57 ± 142.49b	407.46 ± 12.57a	498.11 ± 30.76a	343.32 ± 0.20a	342.45 ± 33.37a	686.16 ± 140.33b	184.20 ± 9.65a

Different letters at the same day column for the parameters from different treatment group represent significant difference at the 0.05 significance level (Tukey HSD), mean values ±SD, n = 3.

Analysis of the changes in the chlorophyll *a* content revealed that the photosynthetic systems of the leaf cells of *M. spicatum* apical fragments were inhibited after the first day. On day 3, significant changes started to occur between T3 and CG ($P < 0.01$, Bonferroni). Compared to that in CG, the chlorophyll *a* decline in T3 was the largest, followed by that in T2 and then T1. However, on day 5, the contents of chlorophyll *a* was shown to increase in all the different treatment groups, but the chlorophyll *a* contents in T1, T2, and T3 were still low compared to that in CG, 4.37%, 5.68%, and 21.43% lower, respectively (Figure 3).

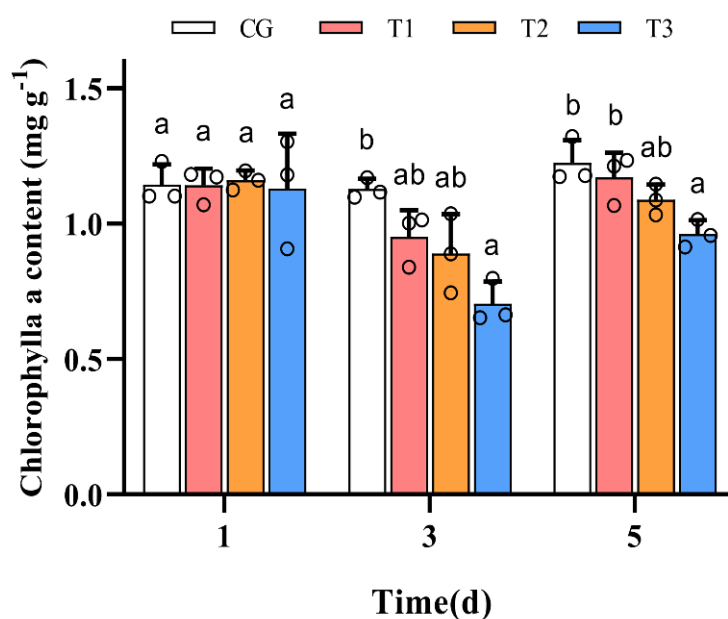


Figure 3. Chlorophyll *a* content for *M. spicatum* in each treatment on day 1, 3, and 5 (data points). CG: control group; T1: 0.1 times of original decomposing liquid; T2: 0.2 times of original decomposing liquid; T3: 0.4 times of original decomposing liquid. Error bars represent standard deviation ($n = 3$). Different letters on top of column indicate significant differences among treatments at the 0.05 significance level (Tukey HSD). Each dot represents a replicate.

3.3. Change of the Soluble Sugars Content

The soluble sugar contents in the treatment groups showed significant differences on the first day. With increasing treatment concentration, the soluble sugar content of the leaves of the *M. spicatum* apical fragments improved, and the soluble sugar content was the highest in T3. Thereafter, the soluble sugar contents gradually dropped during the experiment in T1 and T2. However, it continuously increased in T3, increasing by 115.26% relative to the control, and reaching its highest value on day 5 ($P < 0.05$, Bonferroni) (Figure 4).

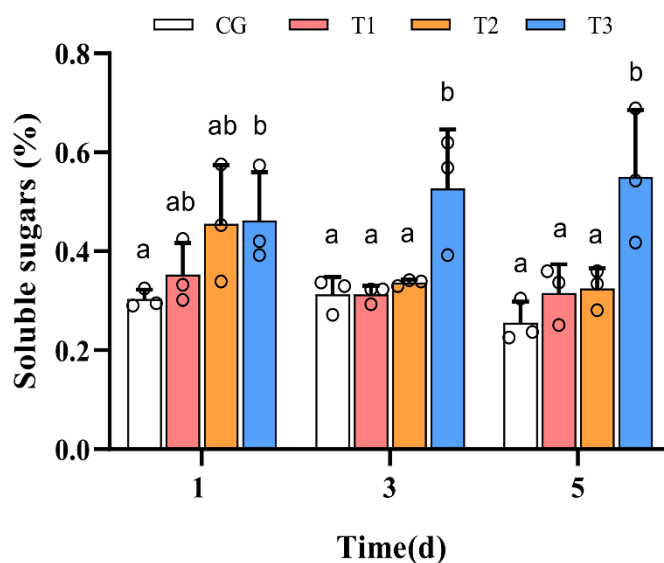


Figure 4. The content of soluble sugars for *M. spicatum* in each treatment on day 1, 3, and 5 (data points). CG: control group; T1: 0.1 times of original decomposing liquid; T2: 0.2 times of original decomposing liquid; T3: 0.4 times of original decomposing liquid. Error bars represent standard deviation ($n = 3$). Different letters on top of column indicate significant differences among treatments at the 0.05 significance level (Tukey HSD). Each dot represents a replicate.

3.4. Changes in Activities of $\text{Ca}^{2+}/\text{Mg}^{2+}$ -ATPase and PAL

The $\text{Ca}^{2+}/\text{Mg}^{2+}$ -ATPase activity in CG did not show significant changes during the experimental period whereas in T3 it was higher than it was in the other treatment groups from the first day. On day 3, these differences gradually increased with increasing concentration, especially between T2 (T3) and CG ($P < 0.001$, $P < 0.001$, Bonferroni). The activities in the treatment groups were significantly increased by 306.25% (T1), 428.13% (T2), and 490.63% (T3) relative to those of CG on day 5 ($P < 0.001$, $P < 0.001$, Bonferroni) (Figure 5A).

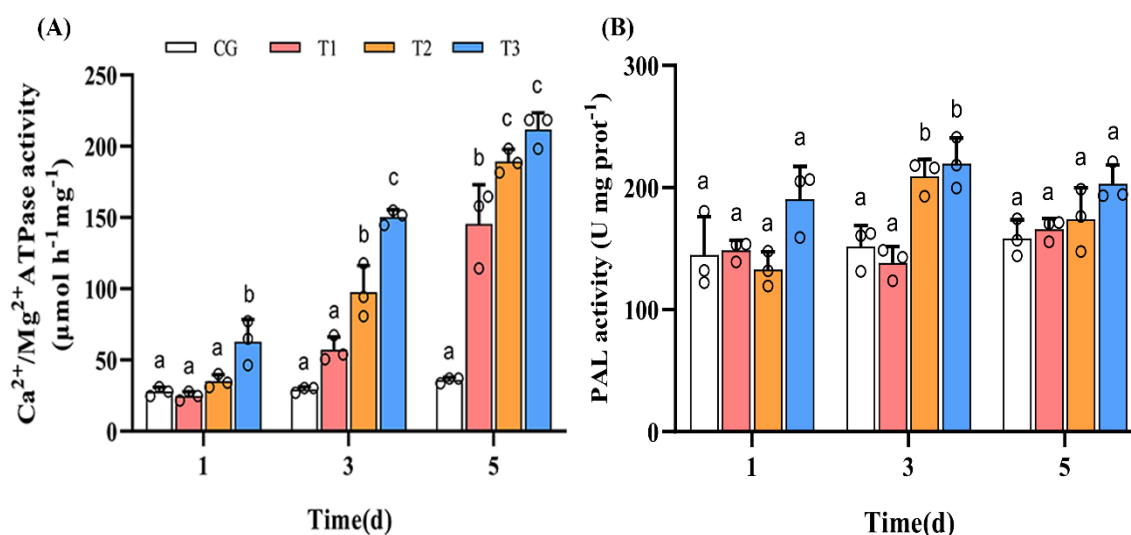


Figure 5. Changes of activities of $\text{Ca}^{2+}/\text{Mg}^{2+}$ -ATPase (A) and PAL (B) for *M. spicatum* in each treatment on day 1, 3, and 5 (data points). CG: control group; T1: 0.1 times of original decomposing liquid; T2: 0.2 times of original decomposing liquid; T3: 0.4 times of original decomposing liquid. Different letters on top of column indicate significant differences among treatments at the 0.05 significance level (Tukey HSD). Each dot represents a replicate.

From Figure 5B, it can be seen that the PAL activities in CG and T1 showed no significant changes during the experimental period. The differences between the treatment group and CG on the first and fifth days were also not obvious. Nevertheless, the PAL activities in the higher concentration treatments (T2 and T3) were activated from day 1 and then slightly inhibited from day 3. The differences between T2 (T3) and CG were significant ($P < 0.05$, $P < 0.01$, Bonferroni). Compared with CG, the PAL activity in T1, T2, and T3 on day 5 increased by 4.65%, 9.91%, and 28.13%, respectively.

3.5. Change of Water Quality Parameters in the Culture Solution

The changes in the DO in each treatment group (shown in Table 3) indicated that, as the experiment progressed, each treatment group showed a certain amount of recovery in terms of dissolved oxygen, compared with CG ($P < 0.001$, $P < 0.001$, $P < 0.01$, ANOVA). DO in T1 gradually increased during the experiment, and the dissolved oxygen level was similar to CG on day 5. The increase in dissolved oxygen in T2 was not as effective as that in T1, and the DO value on day 5 was still lower than those in CG and T1. The DO in the highest concentration decomposing solution (T3) rose until day 3 and then began to decline. It was also low by the end of the experiment. The difference between T2 (T3) and CG was most significant on day 1 ($P < 0.001$, $P < 0.001$, Bonferroni) followed by the differences between T3 and CG on day 3 and day 5 ($P < 0.001$, $P < 0.001$, Bonferroni). For the Cond, after the addition of the decomposing solution in each treatment group, the intensity of the Cond changed with the concentration of the decomposing liquid, and T3 was the highest. Although there was a tendency in T3 for Cond to decrease with time during the experiment, it still maintained a high Cond after 5 days. There was no significant change in Cond in either CG or T1, while the Cond in T2 increased slightly on day 5. Significant differences occurred between the treatment groups and CG during the experiment ($P < 0.001$, $P < 0.001$, $P < 0.001$, Bonferroni). Similar to DO, the pH of each treatment group changed over time, and the differences with time in T1 and T3 were significant ($P < 0.05$, $P < 0.05$, ANOVA). However, on day 5, the pH of each treatment group was still lower than that of CG; 3.90%, 7.79%, and 8.15% lower than the CG, respectively.

Table 3. Monitoring data of pH, DO, and Cond in culture solution.

Treatment	DO (mg L ⁻¹)			Cond (μs cm ⁻¹)			pH		
	1d	3d	5d	1d	3d	5d	1d	3d	5d
CG	11.29 ± 0.58c	11.29 ± 1.47d	11.89 ± 0.61c	370.93 ± 0.75a	369.17 ± 2.65a	370.80 ± 2.95a	9.01 ± 0.09b	9.02 ± 0.28b	9.16 ± 0.15b
T1	1.78 ± 0.70b	8.72 ± 0.50c	11.45 ± 1.36c	609.20 ± 6.70b	609.43 ± 10.05b	602.70 ± 17.21b	8.27 ± 0.06a	8.48 ± 0.10a	8.80 ± 0.24ab
T2	0.12 ± 0.04a	3.70 ± 0.66b	8.20 ± 1.38b	817.67 ± 6.35c	815.57 ± 5.12c	824.73 ± 11.99c	8.33 ± 0.12a	8.39 ± 0.09a	8.44 ± 0.06a
T3	0.01 ± 0.00a	0.49 ± 0.14a	0.33 ± 0.08a	1253.67 ± 17.04d	1229.67 ± 19.73d	1222 ± 14.53d	8.05 ± 0.16a	8.34 ± 0.09a	8.41 ± 0.20a

Different letters in the same day column for the parameters from different treatment group represent significant difference at the 0.05 significance level (Tukey HSD), mean values ±SD, n = 3.

3.6. Result of RDA Sorting

RDA was carried out on the physiological and biochemical characteristics of the *M. spicatum* apical fragments and three water quality parameters. First, the three water quality parameters were used to explain the physiological and biochemical characteristics of the apical fragments (Table 4). The physiological and biochemical characteristics of the apical fragment could explain 82.90% and 11.40% of the variation on the first and second axes, respectively. The cumulative interpretation of the physiological and biochemical characteristics of the apical fragments was 94.30%, and the cumulative interpretation of the relationship between the physiological and biochemical characteristics and the water quality parameters was as high as 99.80%. The first two axes could, therefore, reflect the variation in the physiological and biochemical characteristics of the apical fragments and water quality parameters well. The relationship was mainly determined by Axis I. The correlation coefficients for the relationships between the water quality parameters and each sorting axis are shown in Table 5. Among the three water quality parameters, the correlation coefficient for Cond and the first axis is the largest, reaching 0.9963, and showing a positive correlation, which explains that the first axis reflects the influence of conductivity. The correlation coefficient for pH and the second axis is the largest (−0.4212) and is negatively correlated indicating that the second axis reflects the influence of pH. The third axis also mainly reflects the influence of pH. The correlation between the fourth axis and the three water quality parameters is small. It further obtained a two-dimensional sorting map of the physiological and biochemical characteristics of the apical fragment and water quality parameters (Figure 6). In the sorting diagram, the length of the arrow indicates the relationship between the physiological and biochemical characteristics of the apical fragments and the water quality parameters. The longer the connection arrow, the greater the correlation, and the smaller the angle between the arrow and the sorting axis, the greater the correlation. It can be seen from Figure 6 that the arrow connecting Cond and DO is the longest, and that Cond and DO explain the changes in the physiological and biochemical characteristics of the apical fragments well. Cond is directly proportional to $\text{Ca}^{2+}/\text{Mg}^{2+}$ -ATPase, PAL, and soluble sugar content, and is most highly correlated with PAL. The soluble sugar content was inversely proportional to the other physiological and biochemical indicators of the apical fragment. However, both DO and pH were negatively correlated with $\text{Ca}^{2+}/\text{Mg}^{2+}$ -ATPase, PAL, and soluble sugar content; and positively correlated with Chlorophyll *a* content, root length, root number, bud number, and the two partial photosynthetic parameters (F_v/F_m , PI_{ABS}).

Based on these results, it can be concluded that the influence of water quality parameters on the physiological and biochemical characteristics of apical fragments differs. The Monte Carlo test was carried out on the three water quality parameters, and the order of importance of the water quality environmental variables was obtained. The results are shown in Table 6. The order of importance of the water quality parameters on branching was (from most to least important): Cond, DO, and pH. Their effects on the physiological and biochemical characteristics of the apical fragments were extremely significant ($P < 0.01$), and Cond accounted for 82.50% of all environmental factors, indicating that Cond is the most important factor affecting the physiological and biochemical characteristics of apical fragments.

Table 4. The RDA (redundancy analysis) of the physiological and biochemical characteristics of *M. spicatum* apical fragment.

Axis	Axis I	Axis II	Axis III	Axis IV
Variance explains of characteristics	82.9	11.4	0.2	2.6
Correlations between physiological and biochemical characteristics and water quality parameters	0.999	0.940	0.340	0.000
Cumulative percentage variance of physiological and biochemical characteristics	82.9	94.2	94.4	97.0
Cumulative percentage variance of relation between physiological and biochemical characteristics and water quality parameters	87.8	99.8	100.0	0.0
Sum of all canonical eigenvalues		0.944		
Sum of all eigenvalues		1.000		

Table 5. Correlation of water quality parameters with the axes.

Water Quality Parameters	Axis I	Axis II	Axis III	Axis IV
DO	−0.9683	0.2140	0.0323	0.0000
pH	−0.8067	−0.4212	0.1327	0.0000
Cond	0.9963	0.0607	0.0128	0.0000

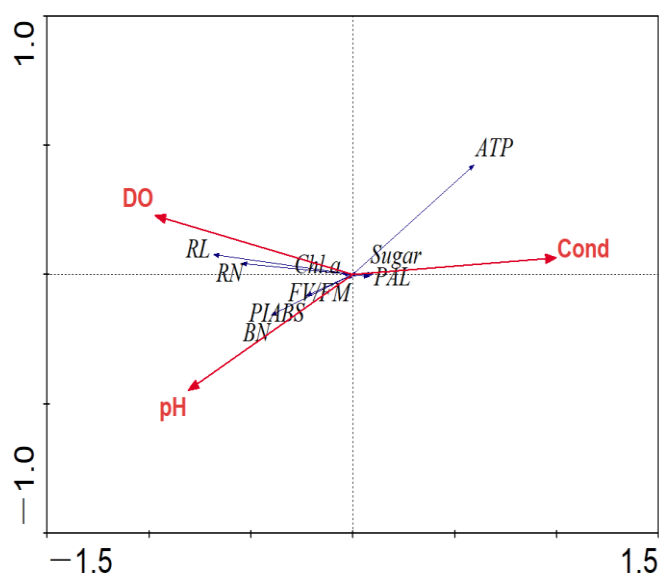


Figure 6. Biplot of the first two axes of the RDA (redundancy analysis) for water quality parameters associated with physiological and biochemical characteristics of *Myriophyllum spicatum*. The abbreviations are—RL: root length; RN: root number; BN: bud number; ATP: $\text{Ca}^{2+}/\text{Mg}^{2+}$ -ATPase; DO: dissolved oxygen; Cond: conductivity; pH: pH; Sugar: soluble sugar; Chl.a: chlorophyll *a*; PAL: PAL; FV/FM: F_V/F_M ; PIABS: PI_{ABS} .

Table 6. Importance and signification level of water quality parameters.

Water Quality Parameters	Importance Rank	Variance Explains of Water Quality Parameters	F	P
Cond	1	82.5	47.004	0.002
DO	2	78.4	36.384	0.002
pH	3	56.3	12.901	0.006

4. Discussion

4.1. Effects on the Photosynthetic System of *M. spicatum* Apical Fragment Leaves

In this study, the chlorophyll *a* content significantly decreased in T3, the treatment with the highest concentration of decomposing liquid, in contrast to the control. Similar results have also been reported by Asaeda et al. [47], who showed that the chlorophyll *a* content of *M. spicatum* declined under high environmental stress. These results suggest that the ability of *M. spicatum* cells to synthesize chlorophyll was reduced in the presence of decomposing liquid, and the lower chlorophyll content in the treatment groups reflected a reduction in the antenna size of the photosynthetic RC complexes and thus their ability to capture light energy declined [48].

The maximum photochemical efficiency (F_V/F_M) of the leaves of *M. spicatum* apical fragments in the treatment groups was lower than that in CG on day 5, which indicates that the initial light energy conversion efficiency of PSII was decreased, and that the potential activity of PSII and the original reaction process of photosynthesis were inhibited. Similar results have been previously reported.

For example, the F_V/F_M values of *Vallisneria natans* fragments also decreased under environmental stress [49]. In contrast to F_V/F_M , PI_{ABS} is a more sensitive photosynthetic parameter that reflects the state of the photosynthetic system and can detect plant stress even before significant symptoms appear on the leaf [50,51]. The significant decreases of PI_{ABS} in T2 and T3 mean visible vitality losses in PSII [52].

The rapid chlorophyll fluorescence induction curves of plants contain a large amount of information about the primary photochemical reaction of the PSII reaction center [53]. By analyzing the curve fluorescence parameters (Table 2), changes in the photosynthetic apparatus of plant materials under the influence of environmental factors can be explored. As the concentration of the decomposing liquid increased, the V_J and M_o values of *M. spicatum* showed higher increases after 5 days, indicating an increase in the degree of closure of the PSII reaction center. More of the Q_A was in a reduced state, resulting in a large amount of Q_A^- accumulating, which prevented it from transmitting electrons. The electron transport chain on the receptor side of the PSII reaction center was inhibited, leading to a significant decrease in ψ_o and ϕ_{Eo} , and a decline in the electron transport abilities of the leaves of *M. spicatum*. In the present study, the ABS/RC and TR_o/RC parameters reached their maximum values on the third day and then decreased in CG and T1. The ABS/RC and TR_o/RC parameters in T2 and T3 continued to rise throughout the experiment. The ET_o/RC and DI_o/RC in T2 and T3 also showed increasing trends, whereas the change in RC/CS was the opposite. These results further indicate that the presence of the decomposing liquid led to a decrease in the light utilization ability of the *M. spicatum* apical fragments, and that their PSII function was blocked, inactivating some of the PSII reaction centers. The energy flow changed, the unit reaction center and energy per unit area for heat dissipation increased significantly, and conversely, the energy used for electron transport and delivery to the end of the electron chain was significantly reduced. Consistent with our hypothesis, it deduced that the photosynthetic system of the apical fragments of *M. spicatum* showed a certain degree of damage under the environmental stress caused by the decomposing liquid, and the differences became more significant as the concentration of the decomposing solution increased.

4.2. Physiological and Biochemical Response of *M. spicatum* Apical Fragments

Soluble sugar is an important product of plant photosynthesis that is mobilized to precipitate tissues to support plant growth and differentiation. It is also a signal that controls various metabolic and developmental processes [54]. Our results show that the cumulative soluble sugar content of apical fragment leaves treated with the highest concentration of the decomposing liquid was always significantly higher than that of the other treatment groups and the control group by the end of the experiment. Similar studies have also reported that the soluble sugar content of *M. spicatum* fragments was elevated in under high nutrient stress [55]. These results indicate that under the stress of a high concentration of decomposing liquid, the survival strategy of *M. spicatum* apical fragments was to accumulate more sugar to cope with the stress. Meanwhile, the sugar acted as a metabolic regulation signal leading to reduced chlorophyll content and photosynthesis and resulting in partial leaves becoming senescent and falling off [56,57].

In accordance with previous studies reported by Ahmed et al. [58] and Ye et al. [59], the Ca^{2+}/Mg^{2+} -ATPase activity of plants increased significantly under environmental stress. The increasing Ca^{2+}/Mg^{2+} -ATPase activity suggests that the ATPase activity in *M. spicatum* apical fragments is related to their tolerance to decomposing liquid. Thus, the change of Ca^{2+}/Mg^{2+} -ATPase activity indicates an alteration in membrane function, as the decomposing liquid may cause damage to cell membrane structure and change the permeability of the cell membrane, inducing the leakage of intracellular matter and even leading to cell death. In addition, it consider that the enhancement of the Ca^{2+}/Mg^{2+} -ATPase may also be an emergency mechanism of cellular metabolism because it can affect the composition and function of the PSII center and hinder electron transport in PSII, thereby inducing more ATP synthesis and providing energy for survival under stress for a short period [58,60,61].

Similar to the $\text{Ca}^{2+}/\text{Mg}^{2+}$ -ATPase activity, PAL activity was significantly increased in the highest concentration of the decomposing liquid. The result imply that increased PAL activity may lead to biosynthesis-related secondary metabolites, which might be a defense response in *M. spicatum* [62,63]. For example, the secondary metabolite lignin can bind to extracellular substances to reduce and eliminate the effects of environmental stress on plants [64].

4.3. Effects on Water Quality and Morphological Characteristics of *M. spicatum* Apical Fragments

Under environmental stress conditions, the physiological and biochemical characteristics of *M. spicatum* apical fragments underwent a series of changes, which in turn affected the morphology and regenerative capacity of the fragments. [65]. For rooted species, whether the plant fragment can continue rooting and germination is an important aspect in determining whether the fragment successfully regenerates in a new environment [66,67]. Consistent with previous research that reported that water quality (e.g., DO, pH, and nutrients) changes during the decomposition of algae [68,69], our results showed that the dissolved oxygen and conductivity of the culture solution treated with the decomposing liquid underwent tremendous changes in a short period of time. Furthermore, some harmful organic substances—such as phenolic acid and toxic aromatic compounds—could be released during algae decomposition, which is not conducive to submerged macrophyte growth [12,17]. Generally, the decomposition of the organic matter in algae produces organic acid compounds consumes oxygen and creates a large amount of carbon dioxide, causing the pH of the water to decrease. This was observed after the decomposition solution was added to the culture solution [15,70]. However, there were no significant changes in the pHs of the treatment groups in this study. This is due to the lower CO_2 compensation point of *M. spicatum*, which can utilize lower levels of CO_2 . This ability to withstand pH changes means that a decline in pH value will have little effect on *M. spicatum* [71,72]. In the treatments with higher decomposing liquid concentrations, an anoxic ($<0.5 \text{ mg}\cdot\text{L}^{-1}$) and high conductivity ($1222 \pm 14.53 - 1253.67 \pm 17.04 \mu\text{s}\cdot\text{cm}^{-1}$) environment was created. The high conductivity means a high concentration of electrolytes and indicates abundant organic matter and nutrients [73]. Based on these observations, further analysis of the relationship between the physiological and biochemical characteristics of apical fragments and water quality parameters also found that the correlation between Cond, DO, pH, and the physiological and biochemical characteristics of apical fragment were significant, indicating that these three water quality parameters were common influencers of the responses of apical fragments under environmental stress. Among them, Cond accounted for a large amount of the interpretive power, and is consequently the most important factor affecting the physiological and biochemical changes in apical fragments. The high conductivity also confirmed that the ion concentration increased, the permeability of the cell membranes changed, and the transport balance of Ca^{2+} was disrupted, in turn causing $\text{Ca}^{2+}/\text{Mg}^{2+}$ -ATPase activity to increase.

Our experimental results demonstrate that *M. spicatum* apical fragments were not only prevented from absorbing normal nutrients for growth under higher decomposing liquid concentrations but were also inhibited during regeneration, which was reflected in their inability to grow roots and buds.

4.4. Summary

This research consider that the main reason behind the *M. spicatum* apical fragments' failures in rooting and sprouting due to the decomposition liquid of *C. oligoclona* is the sudden changes in water quality, which reduce dissolved oxygen and produce more harmful organic substances. It found that higher conductivity in the environment greatly affects the physiological and biochemical characteristics of apical fragments. This gives rise to a series of physiological and biochemical responses in the fragments, resulting in the photosynthetic system, the chlorophyll content, and the activity of the PSII photoreaction center being reduced, electron transfer being hindered, and consequently, the photosynthetic system being damaged. In response to the environmental stresses caused by the decomposing liquid, relevant sugar accumulated in the metabolic system and an energy enzyme and a secondary metabolic-related enzyme were activated as a defense. These findings reveal and explain

the physiological and biochemical aspects of submerged macrophyte apical fragment responses to regenerative resistance, and suggest a focus on regulating the excessive growth of FGA. This would be beneficial in improving the regeneration rate of submerged macrophyte fragments during the restoration of aquatic vegetation to achieve more efficient recovery and improve management of the aquatic environment.

Author Contributions: Writing-Original Draft Preparation, Methodology, Formal Analysis, L.Z.; Software, Investigation, S.H. and X.P.; Conceptualization, Writing-Review & Editing, B.L.; Visualization, Y.Z.; Project Administration, Q.Z.; Supervision, Z.W.

Funding: This study was supported by the National Nature Science Foundation of China (grant number 31830013), the State Key Laboratory of Freshwater Ecology and Biotechnology (grant number 2017FB05) and the Key Research and Development Plan of Ningxia Hui Autonomous Region (grant number 2017BY087).

Acknowledgments: The help and guidance of Yongyuan Zhang in the manuscript preparation and experimental work is gratefully acknowledged.

Conflicts of Interest: The authors declare no conflict of interest.

References

1. Zhang, M.; Dolatshah, A.; Zhu, W.; Yu, G. Case Study on Water Quality Improvement in Xihu Lake through Diversion and Water Distribution. *Water* **2018**, *10*, 333. [[CrossRef](#)]
2. Le Moal, M.; Gascuel-Oudou, C.; Ménesguen, A.; Souchon, Y.; Étrillard, C.; Levain, A.; Moatar, F.; Pannard, A.; Souchu, P.; Lefebvre, A.; et al. Eutrophication: A new wine in an old bottle? *Sci. Total Environ.* **2019**, *651*, 1–11. [[CrossRef](#)]
3. Qin, B.Q.; Gao, G.; Zhu, G.W.; Zhang, Y.L.; Song, Y.Z.; Tang, X.M.; Xu, H.; Deng, J.M. Lake eutrophication and its ecosystem response. *Chin. Sci. Bull.* **2013**, *58*, 961–970.
4. Ibelings, B.W.; Portielje, R.; Lammens, E.H.; Noordhuis, R.; van den Berg, M.S.; Joosse, W.; Meijer, M.L. Resilience of alternative stable states during the recovery of shallow lakes from eutrophication: Lake Veluwe as a case study. *Ecosystems* **2007**, *10*, 4–16. [[CrossRef](#)]
5. Gu, J.; He, H.; Jin, H.; Yu, J.; Jeppesen, E.; Nairn, R.W.; Li, K. Synergistic negative effects of small-sized benthivorous fish and nitrogen loading on the growth of submerged macrophytes—Relevance for shallow lake restoration. *Sci. Total Environ.* **2018**, *610*, 1572–1580. [[CrossRef](#)] [[PubMed](#)]
6. Combroux, I.C.S.; Bornette, G. Propagule banks and regenerative strategies of aquatic plants. *J. Veg. Sci.* **2004**, *15*, 13–20. [[CrossRef](#)]
7. Zhou, Y.W.; Zhou, X.H.; Han, R.M.; Xu, X.G.; Wang, G.X.; Liu, X.S.; Bi, F.Z.; Feng, D.Y. Reproduction capacity of *Potamogeton crispus* fragments and its role in water purification and algae inhibition in eutrophic lakes. *Sci. Total Environ.* **2017**, *580*, 1421–1428. [[CrossRef](#)]
8. Cao, Q.J.; Wang, D. Fragment growth of rooted and rootless submerged aquatic macrophytes: Effects of burial modes and decapitation of shoot apex. *J. Freshw. Ecol.* **2012**, *27*, 315–324. [[CrossRef](#)]
9. Bakker, E.S.; Van Donk, E.; Declerck, S.A.J.; Helmsing, N.R.; Hidding, B.; Nolet, B.A. Effect of macrophyte community composition and nutrient enrichment on plant biomass and algal blooms. *Basic Appl. Ecol.* **2010**, *11*, 432–439. [[CrossRef](#)]
10. Irfanullah, H.M.; Moss, B. Factors influencing the return of submerged plants to a clear-water, shallow temperate lake. *Aquat. Bot.* **2004**, *80*, 177–191. [[CrossRef](#)]
11. Rodrigo, M.A.; Rojo, C.; Alonso-Guillén, J.L.; Vera, P. Restoration of two small Mediterranean lagoons: The dynamics of submerged macrophytes and factors that affect the success of revegetation. *Ecol. Eng.* **2013**, *54*, 1–15. [[CrossRef](#)]
12. Gubelit, Y.L.; Berezina, N.A. The causes and consequences of algal blooms: The *Cladophora glomerata* bloom and the Neva estuary (eastern Baltic Sea). *Mar. Pollut. Bull.* **2010**, *61*, 183–188. [[CrossRef](#)]
13. Lee, J.H.; Lee, J. Indole as an intercellular signal in microbial communities. *FEMS Microbiol. Rev.* **2010**, *34*, 426–444. [[CrossRef](#)]
14. Amador-Noguez, D.; Brasg, I.A.; Feng, X.J.; Roquet, N.; Rabinowitz, J.D. Metabolome remodeling during the acidogenic-solventogenic transition in *Clostridium acetobutylicum*. *Appl. Environ. Microbiol.* **2011**, *77*, 7984–7997. [[CrossRef](#)]

15. Peller, J.R.; Byappanahalli, M.N.; Shively, D.; Sadowsky, M.J.; Chun, C.L.; Whitman, R.L. Notable decomposition products of senescing Lake Michigan *Cladophora glomerata*. *J. Gt. Lakes Res.* **2014**, *40*, 800–806. [[CrossRef](#)]
16. Mäemets, H.; Freiberg, L. Long-and short-term changes of the macrophyte vegetation in strongly stratified hypertrophic Lake Verevi. *Hydrobiologia* **2005**, *547*, 175–184. [[CrossRef](#)]
17. Ye, N.H.; Zhang, X.W.; Mao, Y.Z.; Liang, C.W.; Xu, D.; Zou, J.; Zhuang, Z.M.; Wang, Q.Y. 'Green tides' are overwhelming the coastline of our blue planet: Taking the world's largest example. *Ecol. Res.* **2011**, *26*, 477–485. [[CrossRef](#)]
18. Zhang, L.; Peng, X.; Liu, B.; Zhang, Y.; Zhou, Q.; Wu, Z. Effects of the decomposing liquid of *Cladophora oligoclona* on *Hydrilla verticillata* turion germination and seedling growth. *Ecotoxicol. Environ. Safe* **2018**, *157*, 81–88. [[CrossRef](#)]
19. Wang, C.; Liu, S.; Jahan, T.E.; Liu, B.; He, F.; Zhou, Q.; Wu, Z. Short term succession of artificially restored submerged macrophytes and their impact on the sediment microbial community. *Ecol. Eng.* **2017**, *103*, 50–58. [[CrossRef](#)]
20. Xie, D.; Yu, D. Size-related auto-fragment production and carbohydrate storage in auto-fragment of *Myriophyllum spicatum* L. in response to sediment nutrient and plant density. *Hydrobiologia* **2011**, *658*, 221–231. [[CrossRef](#)]
21. Li, F.; Qin, Y.; Zhu, L.; Xie, Y.; Liang, S.; Hu, C.; Chen, X.; Deng, Z. Effects of fragment size and sediment heterogeneity on the colonization and growth of *Myriophyllum spicatum*. *Ecol. Eng.* **2016**, *95*, 457–462. [[CrossRef](#)]
22. Bickel, T.O. Processes and factors that affect regeneration and establishment of the invasive aquatic plant *Cabomba caroliniana*. *Hydrobiologia* **2017**, *788*, 157–168. [[CrossRef](#)]
23. Wang, J.W.; Yu, D.; Wang, Q. Growth, biomass allocation, and autofragmentation responses to root and shoot competition in *Myriophyllum spicatum* as a function of sediment nutrient supply. *Aquat. Bot.* **2008**, *89*, 357–364. [[CrossRef](#)]
24. Xie, D.; Yu, D.; You, W.H.; Wang, L.G. Morphological and physiological responses to sediment nutrients in the submerged macrophyte *Myriophyllum spicatum*. *Wetlands* **2013**, *33*, 1095–1102. [[CrossRef](#)]
25. Silveira, M.J.; Thomaz, S.M.; Mormul, R.P.; Camacho, F.P. Effects of desiccation and sediment type on early regeneration of plant fragments of three species of aquatic macrophytes. *Int. Rev. Hydrobiol.* **2009**, *94*, 169–178. [[CrossRef](#)]
26. Hall, E.R.; DeGroot, B.C.; Fine, M. Lesion recovery of two scleractinian corals under low pH conditions: Implications for restoration efforts. *Mar. Pollut. Bull.* **2015**, *100*, 321–326. [[CrossRef](#)]
27. Xie, D.; Zhou, H.; Ji, H.; Chen, Y.; An, S. Effects of buoyancy and season on turion dispersal of submerged macrophyte *Potamogeton crispus* L. *Clean Soil Air Water* **2015**, *43*, 324–329. [[CrossRef](#)]
28. Heidbüchel, P.; Hussner, A. Fragment type and water depth determine the regeneration and colonization success of submerged aquatic macrophytes. *Aquat. Sci.* **2019**, *81*, 6. [[CrossRef](#)]
29. Zhou, Y.; Lam, H.M.; Zhang, J. Inhibition of photosynthesis and energy dissipation induced by water and high light stresses in rice. *J. Exp. Bot.* **2007**, *58*, 1207–1217. [[CrossRef](#)]
30. Chen, Y.; Zhou, B.; Li, J.; Tang, H.; Tang, J.; Yang, Z. Formation and Change of Chloroplast-Located Plant Metabolites in Response to Light Conditions. *Int. J. Mol. Sci.* **2018**, *19*, 654. [[CrossRef](#)] [[PubMed](#)]
31. Kalaji, H.M.; Bosa, K.; Kościelniak, J.; Żuk-Gołaszewska, K. Effects of salt stress on photosystem II efficiency and CO₂ assimilation of two Syrian barley landraces. *Environ. Exp. Bot.* **2011**, *73*, 64–72. [[CrossRef](#)]
32. Goussi, R.; Manaa, A.; Derbali, W.; Cantamessa, S.; Abdelly, C.; Barbato, R. Comparative analysis of salt stress, duration and intensity, on the chloroplast ultrastructure and photosynthetic apparatus in *Thellungiella salsuginea*. *J. Photochem. Photobiol. B* **2018**, *183*, 275–287. [[CrossRef](#)] [[PubMed](#)]
33. Pande, J.; Mallhi, K.K.; Grover, A.K. Role of third extracellular domain of plasma membrane Ca²⁺-Mg²⁺-ATPase based on the novel inhibitor caloxin 3A1. *Cell Calcium* **2005**, *37*, 245–250. [[CrossRef](#)] [[PubMed](#)]
34. Liu, Z.; Zhou, L.; Liu, D.; Zhu, Q.; Chen, W. Inhibitory mechanisms of *Acacia mearnsii* extracts on the growth of *Microcystis aeruginosa*. *Water Sci. Technol.* **2015**, *71*, 856–861. [[CrossRef](#)]
35. Markou, G.; Nerantzis, E. Microalgae for high-value compounds and biofuels production: A review with focus on cultivation under stress conditions. *Biotechnol. Adv.* **2013**, *31*, 1532–1542. [[CrossRef](#)] [[PubMed](#)]

36. Swarcewicz, B.; Sawikowska, A.; Marczak, Ł.; Łuczak, M.; Ciesiołka, D.; Krystkowiak, K.; Stobiecki, M. Effect of drought stress on metabolite contents in barley recombinant inbred line population revealed by untargeted GC–MS profiling. *Acta Physiol. Plant.* **2017**, *39*, 158. [[CrossRef](#)]
37. Kim, M.S.; Jin, J.S.; Kwak, Y.S.; Hwang, G.S. Metabolic response of strawberry (*Fragaria x ananassa*) leaves exposed to the angular leaf spot bacterium (*Xanthomonas fragariae*). *J. Agric. Food Chem.* **2016**, *64*, 1889–1898. [[CrossRef](#)] [[PubMed](#)]
38. Yang, K.; Dong, J.; Guo, L.L.; Li, G.B. The Population Structure and the Distributing Characteristics of *Cladophora* in the Littoral Zone of Dianchi Lake. *J. Hydroecology* **2013**, *34*, 8–16. (In Chinese)
39. Schansker, G.; Tóth, S.Z.; Strasser, R.J. Methylviologen and dibromothymoquinone treatments of pea leaves reveal the role of photosystem I in the Chl a fluorescence rise OJIP. *Biochim. Biophys. Acta* **2005**, *1706*, 250–261. [[CrossRef](#)] [[PubMed](#)]
40. Pan, X.L.; Zhang, D.Y.; Li, L. Responses of photosystem II of white elm to UV-B radiation monitored by OJIP fluorescence transients. *Russ. J. Plant Physiol.* **2011**, *58*, 864–870. [[CrossRef](#)]
41. Wang, X.K. *Principles and Techniques of Plant Physiological Biochemical Experiment*, 2nd ed.; Higher Education Press: Beijing, China, 2006; pp. 202–207. (In Chinese)
42. Yemm, E.W.; Willis, A.J. The estimation of carbohydrates in plant extracts by anthrone. *Biochem. J.* **1954**, *57*, 508–514. [[CrossRef](#)]
43. Sykłowska-Baranek, K.; Pietrosiuk, A.; Naliwajski, M.R.; Kawiak, A.; Jeziorek, M.; Wyderska, S.; Chinou, I. Effect of L-phenylalanine on PAL activity and production of naphthoquinone pigments in suspension cultures of *Arnebia euchroma* (Royle) Johnst. *In Vitro Cell. Dev. Biol. Plant* **2012**, *48*, 555–564. [[CrossRef](#)] [[PubMed](#)]
44. Lowry, O.H.; Rosebrough, N.J.; Farr, A.L.; Randall, R.J. Protein measurement with the Folin phenol reagent. *J. Biol. Chem.* **1951**, *193*, 265–275. [[PubMed](#)]
45. Lepš, J.; Šmilauer, P. *Multivariate Analysis of Ecological Data Using CANOCO*; Cambridge University Press: Cambridge, UK, 2003.
46. Makarevich, V.; Legendre, P. Nonlinear redundancy analysis and canonical correspondence analysis based on polynomial regression. *Ecology* **2002**, *83*, 1146–1161. [[CrossRef](#)]
47. Asaeda, T.; Rashid, M.H. Effects of turbulence motion on the growth and physiology of aquatic plants. *Limnologia* **2017**, *62*, 181–187. [[CrossRef](#)]
48. Xu, S.; Yang, S.Q.; Yang, Y.J.; Xu, J.Z.; Shi, J.Q.; Wu, Z.X. Influence of linoleic acid on growth, oxidative stress and photosynthesis of the cyanobacterium *Cylindrospermopsis raciborskii*. *N. Z. J. Mar. Freshw. Res.* **2017**, *51*, 223–236. [[CrossRef](#)]
49. Han, Y.Q.; Wang, L.G.; You, W.H.; Yu, H.H.; Xiao, K.Y.; Wu, Z.H. Flooding interacting with clonal fragmentation affects the survival and growth of a key floodplain submerged macrophyte. *Hydrobiologia* **2018**, *806*, 67–75. [[CrossRef](#)]
50. Viljevac, M.; Dugalić, K.; Mihaljević, I.; Šimić, D.; Sudar, R.; Jurković, Z.; Lepeduš, H. Chlorophyll content, photosynthetic efficiency and genetic markers in two sour cherry (*Prunus cerasus* L.) genotypes under drought stress. *Acta Bot. Croat.* **2013**, *72*, 221–235. [[CrossRef](#)]
51. Zhang, M.; Shan, Y.; Kochian, L.; Strasser, R.J.; Chen, G. Photochemical properties in flag leaves of a super-high-yielding hybrid rice and a traditional hybrid rice (*Oryza sativa* L.) probed by chlorophyll a fluorescence transient. *Photosynth. Res.* **2015**, *126*, 275–284. [[CrossRef](#)]
52. Gonzalez-Mendoza, D.; Gil, F.E.Y.; Rodriguez, J.F.; Marin, S.M.A.; Santamaría, J.M.; Zapata-Perez, O. Photosynthetic responses of a salt secretor mangrove, *Avicennia germinans*, exposed to salinity stress. *Aquat. Ecosyst. Health Manag.* **2011**, *14*, 285–290. [[CrossRef](#)]
53. Hill, R.; Ralph, P.J. Photosystem II heterogeneity of in hospite zooxanthellae in scleractinian corals exposed to bleaching conditions. *Photochem. Photobiol.* **2006**, *82*, 1577–1585. [[CrossRef](#)] [[PubMed](#)]
54. Cho, L.H.; Pasriga, R.; Yoon, J.; Jeon, J.S.; An, G. Roles of Sugars in Controlling Flowering Time. *J. Plant Biol.* **2018**, *61*, 121–130. [[CrossRef](#)]
55. Xie, D.; Yu, D.; You, W.H.; Xia, C.X. The propagule supply, litter layers and canopy shade in the littoral community influence the establishment and growth of *Myriophyllum aquaticum*. *Biol. Invasions* **2013**, *15*, 113–123. [[CrossRef](#)]
56. Yin, L.; Wang, S.; Liu, P.; Wang, W.; Cao, D.; Deng, X.; Zhang, S. Silicon-mediated changes in polyamine and 1-aminocyclopropane-1-carboxylic acid are involved in silicon-induced drought resistance in *Sorghum bicolor* L. *Plant Physiol. Biochem.* **2014**, *80*, 268–277. [[CrossRef](#)] [[PubMed](#)]

57. Wingler, A. Transitioning to the next phase: The role of sugar signaling throughout the plant life cycle. *Plant Physiol.* **2018**, *176*, 1075–1084. [[CrossRef](#)]
58. Ahmed, I.M.; Dai, H.; Zheng, W.; Cao, F.; Zhang, G.; Sun, D.; Wu, F. Genotypic differences in physiological characteristics in the tolerance to drought and salinity combined stress between Tibetan wild and cultivated barley. *Plant Physiol. Biochem.* **2013**, *63*, 49–60. [[CrossRef](#)] [[PubMed](#)]
59. Ye, Z.; Zeng, J.; Li, X.; Zeng, F.; Zhang, G. Physiological characterizations of three barley genotypes in response to low potassium stress. *Acta Physiol. Plant.* **2017**, *39*, 232. [[CrossRef](#)]
60. Huang, H.; Liu, X.; Qu, C.; Liu, C.; Chen, L.; Hong, F. Influences of calcium deficiency and cerium on the conversion efficiency of light energy of spinach. *Biometals* **2008**, *21*, 553–561. [[CrossRef](#)]
61. Fonseca, J.S.; Marangoni, L.F.B.; Marques, J.A.; Bianchini, A. Effects of increasing temperature alone and combined with copper exposure on biochemical and physiological parameters in the zooxanthellate scleractinian coral *Mussismilia harttii*. *Aquat. Toxicol.* **2017**, *190*, 121–132. [[CrossRef](#)]
62. Song, Y.; Chen, D.; Lu, K.; Sun, Z.; Zeng, R. Enhanced tomato disease resistance primed by arbuscular mycorrhizal fungus. *Front. Plant Sci.* **2015**, *6*, 786. [[CrossRef](#)]
63. Chen, Y.; Li, F.; Tian, L.; Huang, M.; Deng, R.; Li, X.; Chen, W.; Wu, P.; Li, M.; Jiang, H.; et al. The phenylalanine ammonia lyase gene LJPAL1 is involved in plant defense responses to pathogens and plays diverse roles in *Lotus japonicus*-rhizobium symbioses. *Mol. Plant Microbe Interact.* **2017**, *30*, 739–753. [[CrossRef](#)] [[PubMed](#)]
64. Pawlak-Sprada, S.; Arasimowicz-Jelonek, M.; Podgórska, M.; Deckert, J. Activation of phenylpropanoid pathway in legume plants exposed to heavy metals. Part I. Effects of cadmium and lead on phenylalanine ammonia-lyase gene expression, enzyme activity and lignin content. *Acta Biochim. Pol.* **2011**, *58*, 211–216. [[CrossRef](#)] [[PubMed](#)]
65. Xie, D.; Yu, D.; Yu, L.F.; Liu, C.H. Asexual propagations of introduced exotic macrophytes *Elodea nuttallii*, *Myriophyllum aquaticum*, and *M. propinquum* are improved by nutrient-rich sediments in China. *Hydrobiologia* **2010**, *655*, 37–47. [[CrossRef](#)]
66. Riis, T. Dispersal and colonisation of plants in lowland streams: Success rates and bottlenecks. *Hydrobiologia* **2008**, *596*, 341–351. [[CrossRef](#)]
67. Umetsu, C.A.; Evangelista, H.B.A.; Thomaz, S.M. The colonization, regeneration, and growth rates of macrophytes from fragments: A comparison between exotic and native submerged aquatic species. *Aquat. Ecol.* **2012**, *46*, 443–449. [[CrossRef](#)]
68. Gao, L.; Zhang, L.; Hou, J.; Wei, Q.; Fu, F.; Shao, H. Decomposition of macroalgal blooms influences phosphorus release from the sediments and implications for coastal restoration in Swan Lake, Shandong, China. *Ecol. Eng.* **2013**, *60*, 19–28. [[CrossRef](#)]
69. Wang, J.Z.; Jiang, X.; Zheng, B.H.; Chen, C.X.; Kang, X.M.; Zhang, C.Y.; Song, Z.Q.; Wang, K.; Wang, W.W.; Wang, S.H. Effect of algal bloom on phosphorus exchange at the sediment–water interface in Meiliang Bay of Taihu Lake, China. *Environ. Earth Sci.* **2016**, *75*, 57. [[CrossRef](#)]
70. Garcia-Robledo, E.; Corzo, A.; De Lomas, J.; Van Bergeijk, S. Biogeochemical effects of macroalgal decomposition on intertidal microbenthos: A microcosm experiment. *Mar. Ecol. Prog. Ser.* **2008**, *356*, 139–151. [[CrossRef](#)]
71. Stanley, R.A.; Naylor, A.W. Photosynthesis in Eurasian watermilfoil (*Myriophyllum spicatum* L.). *Plant Physiol.* **1972**, *50*, 149–151. [[CrossRef](#)]
72. Hussner, A.; Mettler-Altman, T.; Weber, A.P.; Sand-Jensen, K. Acclimation of photosynthesis to supersaturated CO₂ in aquatic plant bicarbonate users. *Freshw. Biol.* **2016**, *61*, 1720–1732. [[CrossRef](#)]
73. Batish, D.R.; Kaur, S.; Singh, H.P.; Kohli, R.K. Role of root-mediated interactions in phytotoxic interference of *Ageratum conyzoides* with rice (*Oryza sativa*). *Flora* **2009**, *204*, 388–395. [[CrossRef](#)]

